

A fractionation approach applying chelating magnetic nanoparticles to characterize pericardial fluid's proteome



Fábio Trindade ^{a, b, *}, Paulo Bastos ^a, Adelino Leite-Moreira ^b, Bruno Manadas ^c, Rita Ferreira ^d, Sofia F. Soares ^e, Ana L. Daniel-da-Silva ^e, Inês Falcão-Pires ^b, Rui Vitorino ^{a, b}

^a iBiMED – Institute of Biomedicine, Department of Medical Sciences, University of Aveiro, Aveiro, Portugal

^b Unidade de Investigação Cardiovascular, Departamento de Cirurgia e Fisiologia, Universidade do Porto, Porto, Portugal

^c CNC – Center for Neuroscience and Cell Biology, University of Coimbra, UC Biotech, Parque Tecnológico de Cantanhede, Portugal

^d QOPNA, Mass Spectrometry Center, Department of Chemistry, University of Aveiro, Aveiro, Portugal

^e CICECO – Aveiro Institute of Materials, Department of Chemistry, University of Aveiro, Aveiro, Portugal

ARTICLE INFO

Article history:

Received 26 April 2017

Received in revised form

18 September 2017

Accepted 20 September 2017

Available online 23 September 2017

Keywords:

Pericardial fluid

Proteomics

Magnetic nanoparticles

ABSTRACT

Owing to their close proximity, pericardial fluid (PF)'s proteome may mirror the pathophysiological status of the heart. Despite this diagnosis potential, the knowledge of PF's proteome is scarce. Large amounts of albumin hamper the characterization of the least abundant proteins in PF. Aiming to expand PF's proteome and to validate the technique for future applications, we have fractionated and characterized the PF, using N-(trimethoxysilylpropyl)ethylenediamine triacetic acid (EDTA)-functionalized magnetic nanoparticles (NPs@EDTA) followed by a GeLC-MS/MS approach. Similarly to an albumin-depletion kit, NPs@EDTA-based fractionation was efficient in removing albumin. Both methods displayed comparable inter-individual variability, but NPs@EDTA outperformed the former with regard to the protein dynamic range as well as to the monitoring of biological processes. Overall, 565 proteins were identified, of which 297 (>50%) have never been assigned to PF. Moreover, owing to this method's good proteome reproducibility, affordability, rapid automation and high binding ability of NP@EDTA, it bears a great potential towards future clinical application.

© 2017 Elsevier Inc. All rights reserved.

1. Introduction

Pericardial fluid (PF) is a plasma ultrafiltrate enclosed in the pericardial sac, providing lubrication during heartbeat [1]. Albeit not commonly used in the clinical routine, PF in close proximity to the heart, likely holds relevant molecular information, reflecting its

pathophysiological status. Even though, the molecular knowledge of PF is rather scarce. The need for an invasive collection and the ethical restraints of collecting PF from healthy subjects have been probably discouraging its study. However, PF can be easily and safely collected, for instance, from patients undergoing open heart surgery [2]. Furthermore, once it is enriched with many bioactive substances, such as cytokines, growth factors or cardiac hormones, governing heart function by autocrine or paracrine activity, PF provides a direct window to the heart. Therefore, the molecular analysis of PF may be an important tool to address the pathophysiological mechanisms underlying cardiac diseases and, simultaneously, to pinpoint potential therapeutic targets [2,3].

Proteomics provides a reliable approach to study PF because the profiling (and quantification) of biofluid proteins allows us to scrutinize directly the phenotype of diseases. Nonetheless, the proteomic characterization of PF can be challenging. First, the albumin content can be even higher than in plasma (71% versus 62%) [3], thus the probability of albumin masking other less abundant

Abbreviations: BCA, bicinchoninic acid; CAD, coronary artery disease; EDTA, N-(trimethoxysilylpropyl)ethylenediamine triacetic acid; EDTA-TMS, N-(trimethoxysilylpropyl)ethylenediamine triacetate trisodium salt; FA, formic acid; FDR, false discovery rate; FTIR, Fourier Transform Infrared; GO, gene ontology; ID, internal diameter; IDA, information-dependent acquisition; LC, liquid chromatography; MARS, multiple affinity removal system; MES, 2-(N-Morpholino)ethanesulfonic acid; MS, mass spectrometry; PF, pericardial fluid; SDS-PAGE, sodium dodecyl sulfate-polyacrylamide gel electrophoresis; TEM, transmission electron microscopy; TOF, time-of-flight.

* Corresponding author. Fábio Trindade iBiMED – Institute of Biomedicine, Department of Medical Sciences, University of Aveiro, Campus Universitário de Santiago, Agra do Crasto – edifício 30, 3810-193 Aveiro, Portugal.

E-mail address: fabiortindade@ua.pt (F. Trindade).

<https://doi.org/10.1016/j.abbi.2017.09.016>

0003-9861/© 2017 Elsevier Inc. All rights reserved.

proteins needs to be accounted for. Second, PF is expected to bear a high dynamic range of protein concentrations because it is generated by plasma ultrafiltration. The plasma itself displays a range higher than 10^{10} -fold [4]. Third, data integration will be difficult since we have available only one study published so far, reporting the first in-depth proteomic characterization of PF [5]. In that study the first 1000 PF proteins were identified by removing the 14 most abundant proteins (using Agilent's Multiple Affinity Removal System, MARS) and by following a SDS-PAGE-LC-MS/MS approach. Still, the removal of so many proteins, e.g. albumin, IgM or apolipoprotein AI, was made at the expense of other less abundant small proteins/peptides, which bind to the column-captured proteins. Besides, such method is highly expensive due to the antibody dependency, which readily hampers large-scale use in clinical research.

We have previously used magnetic nanoparticles functionalized with N-(trimethoxysilylpropyl)ethylenediamine triacetic acid (EDTA) (NPs@EDTA) to obtain metal-dependent proteins-enriched salivary fraction from chronic periodontitis subjects to perform gelatin zymography. In such assay, NPs@EDTA proved to be useful for metalloproteases enrichment as evidenced by enhanced metalloproteases-driven gelatinolytic activity [6]. The ability to enrich metalloproteins or metal-dependent proteins is explained by the EDTA's chelating properties, a pentadentate ligand anchored in the surface of magnetic nanoparticles. Additionally, these nanoparticles display tremendous potential for clinical application owing to their affordability, high surface area-to-volume ratio and, thus, sensibility, in addition to the ability to provide a fast separation upon application of an external magnetic field [7].

We hypothesized that processing PF with NPs@EDTA would deepen PF's proteome knowledge, by enriching low abundant proteins. Therefore, we aimed to validate the use of NPs@EDTA to fractionate and characterize PF proteome and also to expand the proteome catalogued to date. In order to do that, we have compared the application of these lab-made nanoparticles with a commercial albumin/IgG-depletion kit, with regard to the SDS-PAGE profiles as well as to the profile of protein fractions and to the trackable biological processes.

2. Materials and methods

2.1. Sample collection, processing and protein quantification

PF was collected from two obese, hypertensive and diabetic female patients during valve surgery (samples were named PF1 and PF2). A third sample was collected from an obese, hypertensive non-diabetic male patient during valve surgery (named PF3). Approximately 15 mL of fluid was collected from each patient immediately after sternotomy and pericardiotomy. Following collection, PF was centrifuged at 5000 rpm, 4 °C for 15 min to remove cellular components and the supernatant was stored at -80 °C until further processing. Protein quantification was performed with the BCA protein assay kit (Pierce®, Thermo Scientific). The study was approved by the Institutional Ethical Committee, and all patients provided written informed consent.

2.2. Depletion of albumin and immunoglobulin G from pericardial fluid

PF from subjects PF1 and PF2 was processed using an albumin/IgG-depletion kit (Pierce™ Top 2 Abundant Protein Depletion Spin Columns, Thermo Scientific), according to the manufacturer's protocol. The volume corresponding to 600 µg of proteins was used since the spin columns can process up to 10 µL of serum/plasma (~600 µg of protein). An additional elution step was performed in

order to collect the albumin/IgG-rich fraction. To collect these fractions, samples were incubated with 300 µL of 0.1 M glycine solution pH 2.4, for 30 min, in an end-over-end mixer, and centrifuged for 2 min at $1000 \times g$. Neutralization of samples was achieved with 0.5 M Tris solution pH 8.5.

2.3. Synthesis and characterization of NPs@EDTA

A detailed description of NPs@EDTA (patent register PT107608) preparation has been described elsewhere [7] but, essentially, comprised: i) the synthesis of the magnetic core made of Fe₃O₄ through oxidative hydrolysis of an Iron (II) salt in alkaline medium; ii) surface coating with a shell of amorphous silica (SiO₂) in alkaline environment using tetraethyl *ortho*-silicate as a precursor; and iii) surface chemical functionalization with N-(trimethoxysilylpropyl) ethylenediamine triacetate trisodium salt (EDTA-TMS), as illustrated in Figure S1.

Morphology and size of NPs@EDTA particles were obtained through transmission electron microscopy (TEM) using a Hitachi H-9000 microscope operated at 300 kV. Sample for TEM analysis was prepared by evaporating dilute suspensions of the nanoparticles on a copper grid coated with an amorphous carbon film. The Fourier Transform Infrared (FTIR) spectrum was collected using a spectrometer Mattson 7000 with 256 scans and 4 cm⁻¹ resolution, using a horizontal attenuated total reflectance cell. The surface charge of the NPs was assessed by zeta potential measurements, using a Zetasizer Nanoseries equipment from Malvern Instruments.

2.4. NPs@EDTA assay for fractionation of pericardial fluid proteins

After NPs@EDTA synthesis, a suspension of nanoparticles was prepared in ultrapure water to a known concentration. One mg of NPs@EDTA was used to each sample. Before incubation of samples, magnetic beads were washed with binding buffer [0.01M 2-(N-Morpholino)ethanesulfonic acid (MES), 0.01M NaCl, pH 6.5–8.5]. Then, two independent assays were performed, using samples PF1 and PF2. In the first, 0.6 mg (the same amount processed with the commercial kit) and 3 mg of PF protein were incubated with the beads and subjected to mechanical agitation for 1 h at room temperature. In the second, to estimate NPs@EDTA saturation, 0.3 mg, 1.5 mg, 3 mg and 4.5 mg of PF proteins were incubated with the beads and subjected to the same agitation conditions. After sample incubation, supernatants were collected and the beads were washed 3 times by adding 500 µL of MES buffer and performing agitation cycles for 3–5 min. Elution of beads-bound proteins was carried out with 20 µL of Laemmli loading buffer by promoting further mechanical agitation for 10 min.

2.5. Protein separation by SDS-PAGE

Aiming to compare the protein profiles of the fractions collected with the commercial kit and with the NPs@EDTA, protein fractions were separated by SDS-PAGE, following Laemmli procedure [8]. The volume corresponding to 30 µg of protein from total unprocessed sample and from the protein fractions collected by the commercial kit was directly loaded onto gel. Ten µL of each fraction collected in the first NPs@EDTA assay was also loaded onto gel. This volume was chosen because, when starting with 600 µg of protein, it corresponds to the same protein amount (30 µg) as in the case of the kit. Finally, in the second (saturation) assay the whole adsorbed protein fractions were loaded onto gel. Proteins were separated under reducing and denaturing conditions in 12.5% gels, applying a 200 V voltage. Gels were then incubated in fixation solution (methanol: acetic acid 40:10 v/v) for 45 min, stained with Colloidal Coomassie Blue G250 and destained with 20% methanol until an optimal

contrast was achieved.

2.6. In-gel digestion and peptide clean-up

Each lane of the gels was cut in 16 pieces and washed with 100 mM NH_4HCO_3 and acetonitrile. Proteins were then reduced with dithiothreitol (DTT, 10 mM, 30 min, 60 °C), alkylated in the dark with iodoacetamide (IAA, 55 mM, 30 min, 25 °C) and washed again with 100 mM NH_4HCO_3 and acetonitrile, before being digested with trypsin overnight (37 °C). Peptides were extracted with 10% formic acid (FA), FA 10%: acetonitrile (1:1) and vacuum-dried. Next, peptides were resuspended in 5% acetonitrile and 0.5% trifluoroacetic acid and purified using Pierce® C18 Spin Columns (Thermo Scientific) following the manufacturer's instructions. Peptides were re-dried and kept frozen (−80 °C) until MS-based analysis.

2.7. Reproducibility assay

In order to test the reproducibility of the fractionation method employing magnetic nanoparticles, the third sample (PF3) was processed in duplicate following the same procedure used for the former samples (PF1 and PF2, see section 2.4). Three mg of protein were used as this amount was found to saturate 1 mg of NPs@EDTA. The elution of the proteins bound to the nanoparticles, however, was made with a 50 mM NH_4HCO_3 and 0.1% SDS solution.

2.8. In-solution digestion and peptide clean-up

The protein samples from the reproducibility assay were reduced with DTT (3 μM , 30 min, 56 °C), alkylated in the dark with IAA (5 μM , 30 min, 25 °C) and digested with trypsin overnight at 37 °C, following Wiśniewski et al. [9] FASP procedure. After digestion, peptide mix was acidified with FA and desalted with a MicroSpin C18 column (The Nest Group, Inc) prior to LC-MS/MS analysis.

2.9. Protein identification by LC-MS/MS

Samples from PF1 and PF2 were analyzed on a Triple TOF™ 5600 System (ABSciex®) in information-dependent acquisition (IDA) mode as previously described [10,11]. Peptides were resolved by liquid chromatography (nanoLC Ultra 2D, Eksigent®) on a MicroLC column ChromXP™ C18CL (300 μm internal diameter (ID) \times 15 cm length, 3 μm particles, 120 Å pore size, Eksigent®) at 5 $\mu\text{L}/\text{min}$ with a multistep gradient: 0–2 min linear gradient from 5 to 10%, 2–45 min linear gradient from 10% to 30% and, 45–46 min to 35% of acetonitrile in 0.1% FA. Peptides were ionized into the mass spectrometer using an electrospray ionization source (DuoSpray™ Source, ABSciex®) with a 50 μm ID stainless steel emitter (NewObjective).

For IDA experiments the mass spectrometer was set to scanning full spectra (350–1250 m/z) for 250 ms, followed by up to 100 MS/MS scans (100–1500 m/z from a dynamic accumulation time – minimum 30 ms for precursor above the intensity threshold of 1000 – in order to maintain a cycle time of 3.3 s). Candidate ions with a charge state between +2 and +5 and counts above a minimum threshold of 10 counts/second were isolated for fragmentation and one MS/MS spectra was collected before adding those ions to the exclusion list for 25 s (mass spectrometer operated by Analyst® TF 1.7, ABSciex®). Rolling collision was used with a collision energy spread of 5.

Peptide identification and library generation were performed with Protein Pilot software (v5.1, ABSciex®), using the following parameters: i) search against the SwissProt database (March 2016 release); ii) iodoacetamide as cysteines alkylating agents as fixed

modification; iii) trypsin as digestion type. An independent False Discovery Rate (FDR) analysis using the target-decoy approach provided with Protein Pilot software was used to assess the quality of the identifications and positive identifications were considered when identified proteins and peptides reached a 5% local FDR [12,13].

The peptide mixes from sample PF3 were analyzed using a LTQ-Orbitrap Velos Pro mass spectrometer (Thermo Fisher Scientific, San Jose, CA, USA) coupled to an EasyLC (Thermo Fisher Scientific (Proxeon), Odense, Denmark). Peptides were loaded onto the 2-cm Nano Trap column with an inner diameter of 100 μm packed with C18 particles of 5 μm particle size (Thermo Fisher Scientific) and were separated by reversed-phase chromatography using a 25-cm column with an inner diameter of 75 μm , packed with 1.9 μm C18 particles (Nikkoy Technos Co. Ltd. Japan). Chromatographic gradients started at 93% buffer A and 7% buffer B with a flow rate of 250 nL/min for 5 min and gradually increased 65% buffer A and 35% buffer B in 120 min. After each analysis, the column was washed for 15 min with 10% buffer A and 90% buffer B. Buffer A: 0.1% FA in water. Buffer B: 0.1% FA in acetonitrile.

The mass spectrometer was operated in data dependent acquisition (DDA) mode and full MS scans with 1 micro scans at resolution of 60,000 were used over a mass range of m/z 350–2000 with detection in the Orbitrap. Auto gain control (AGC) was set to 1E6, dynamic exclusion (60 s) and charge state filtering disqualifying singly charged peptides was activated. In each cycle of DDA analysis, following each survey scan the top 20 most intense ions with multiple charged ions above a threshold ion count of 5000 were selected for fragmentation at normalized collision energy of 35%. Fragment ion spectra produced via collision-induced dissociation (CID) were acquired in the Ion Trap, AGC was set to 5e4, isolation window of 2.0 m/z , activation time of 0.1 ms and maximum injection time of 100 ms was used. All data were acquired with Xcalibur software v2.2.

Proteome Discoverer software suite (v1.4, Thermo Fisher Scientific) and the Mascot search engine (v2.5, Matrix Science [14]) were used for peptide identification and quantification. Samples were searched against a SwissProt database containing entries corresponding to human, a list of common contaminants and all the corresponding decoy entries (20797 entries). Trypsin was chosen as enzyme and a maximum of three miscleavages were allowed. Carbamidomethylation (C) was set as a fixed modification, whereas oxidation (M) and acetylation (N-terminal) were used as variable modifications. Searches were performed using a peptide tolerance of 7 ppm, a product ion tolerance of 0.5 Da. Resulting data files were filtered for FDR <5%.

2.10. Proteome analysis, bioinformatics and statistical analysis

The differences between protein profiles were explored by Venn diagram analysis with the help of BioVenn webtool [15], using UniProt accessions.

To determine the cellular localization of the proteins, a STRING [16] analysis was performed. Only GO terms with FDR <0.05 were considered. To get insight into the biological processes that can be screened with both methods, a ClueGO [17] analysis was performed. For the comparison between methodological approaches a 3–8 GO range was set, while GO was fixed on level 3 for the comparison of the experimental dataset to that reported by Xiang's et al. [5] In both cases, only biological processes with a p -value <0.05 were considered.

To estimate the dynamic range of the identified proteins, the base-10 logarithm was calculated, for each protein, from the sum of the peptide intensities and its variation, Δ , was calculated from the difference of the highest and lowest logarithms. To calculate the

dynamic range of the PF proteome already characterized we used the MS/MS raw data available on PRIDE (<http://proteomecentral.proteomexchange.org/cgi/GetDataset>, code PXD000194).

Two-proportion z-test was used to test the representativeness of plasma- and heart-derived proteome to overall PF proteome, in comparison to the aforementioned dataset [5].

3. Results

3.1. Preparation and characterization of NPs@EDTA

The NPs@EDTA were synthesized in three steps (Figure S1), as previously described [7]. TEM analysis (Fig. 1A) shows that these particles present core@shell morphology, comprising a spherical magnetic core of Fe_3O_4 (darker) with an average diameter of 48 ± 8 nm coated with amorphous silica (SiO_2) shells of 14 ± 2 nm in thickness. Owing to Fe_3O_4 core, NPs@EDTA particles are ferromagnetic and display a magnetization hysteresis loop at room temperature (300 K) with small remnant magnetization and coercivity, and a saturation magnetization of 40 emu/g [7]. The FTIR spectrum (Fig. 1B) shows the typical bands of Fe_3O_4 (556 cm^{-1} ($\nu(\text{Fe}-\text{O})$)) and amorphous SiO_2 (1060 cm^{-1} ($\nu_{\text{as}}(\text{SiO}-\text{Si})$), 958 cm^{-1} ($\nu(\text{Si}-\text{OH})$) and 799 and 432 cm^{-1} ($\delta(\text{Si}-\text{O}-\text{Si})$)). Although less intense, the bands at 1386 cm^{-1} ($\nu(\text{C}-\text{OH})$) and 1635 cm^{-1} ($\nu(\text{C}=\text{O})$) support the presence of carboxylic acid groups at the surface of the particles due to the grafting of EDTA-TMS. Accordingly, the surface of NPs@EDTA particles was strongly negatively charged, with zeta potential values of -65.6 mV (pH 7.1, MES buffer).

3.2. SDS-PAGE analysis

After processing PF with the commercial kit, we obtained, for each sample, an albumin/IgG-poor (F1) and rich (F2) fractions. In turn, after fractionating PF with NPs@EDTA we retrieved a non-adsorbed (F3) and an adsorbed (F4) protein fraction. All fractions and the total/unprocessed sample (TF) are depicted in Fig. 2, showing the different protein SDS-PAGE profiles achieved with the depletion (Fig. 2A and B) and the enrichment (Fig. 2C and D) methods. As expected, a dramatic decline in the intensity of the band associated to albumin (~ 69 kDa, HSA in Fig. 2) was found in F1, corroborating albumin removal. In fact, the majority of albumin was captured by the resin antibodies and collected in F2, as shown by increased intensity of albumin's band in the third lane of Fig. 2A and B. Immunoglobulin G removal could also be observed in F1 by a decrease in the intensity of its heavy chain band (IgG h.c. in Fig. 2),

whose weight is known to be close to 50 kDa [18]. Accordingly, the majority of this IgG chain could be seen in F2, where the intensity of the band is identical to the respective in TF. Likewise, by fractionating PF with NPs@EDTA we could get rid of a great amount of albumin and IgG, as corroborated by increased intensity of the respective bands (HSA and IgG h.c.) in F3 (non-adsorbed protein fraction) in comparison to F4 (adsorbed protein fraction), particularly visible when processing 3 mg of protein. Therefore, similarly to the commercial columns, NPs@EDTA offer a platform for the depletion of abundant proteins (albumin and IgG, at least) and concomitant enrichment of low abundant proteins.

3.3. Analysis of proteome coverage, dynamic range and inter-individual variability

A bottom-up approach comprising protein trypsinization and peptide identification by LC-MS/MS was followed. Table 1 summarizes the main proteome data for both methods. Overall, without taking into account the data obtained after performing saturation and reproducibility assays (see sections 3.3. and 3.5), we could identify, on a first analysis, 185 proteins across different samples, fractions and methods (Fig. 3A). From these, 122 proteins (66%) were identified in both subjects (Fig. 3B). Importantly, both depletion and nanoparticles-based methods could increase the number of proteins identified, respectively, by 38% and 40%, over PF's direct analysis. Furthermore, both methods combined increased by 59% the number of identified proteins, showing that depletion of high abundant proteins in PF is imperative to enlarge proteome coverage. Notwithstanding, one should acknowledge that such increase was also a result of the analysis of the albumin/IgG-rich fraction (usually discarded) and of the non-adsorbed protein fraction, which shows that analyzing both fractions in both methods guarantees the deepest proteome coverage (unique contribution of all protein fractions is depicted in Figure S2). While both methods contributed equally to proteome coverage, the same was not true with respect to the protein dynamic range. In fact, NPs@EDTA-based fractionation achieved a higher range of protein abundances (4.5 versus 3.7 log units, Table 2) than the commercial method. Still, such range was found lower when compared to TF (4.8 log units).

With regard to the inter-individual variability, we found that overall subjects shared 66% of the PF proteome and that either processing PF with the kit or with the NPs@EDTA does not induce important variations in the individual proteome, at least, in the desired fractions. In fact, both individuals shared 62% of the proteins in the albumin-poor fraction (F1) and 60% of the proteins in

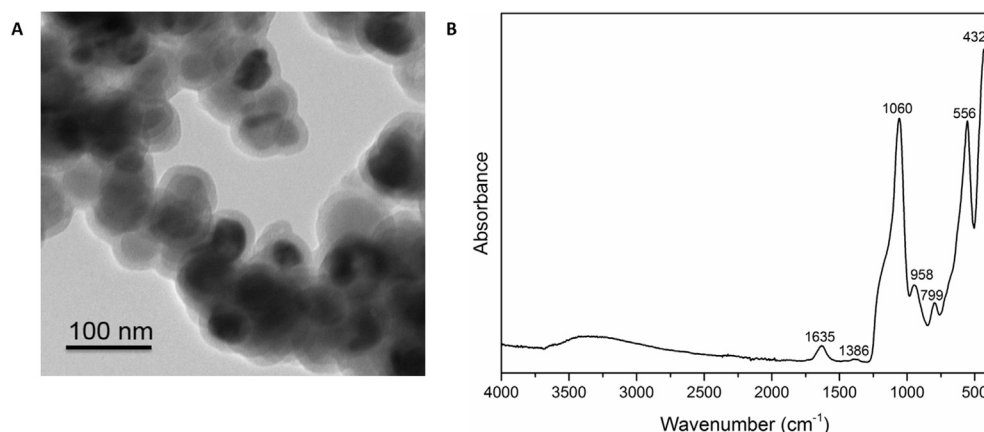


Fig. 1. TEM image (A) and FTIR spectrum (B) of NPs@EDTA.

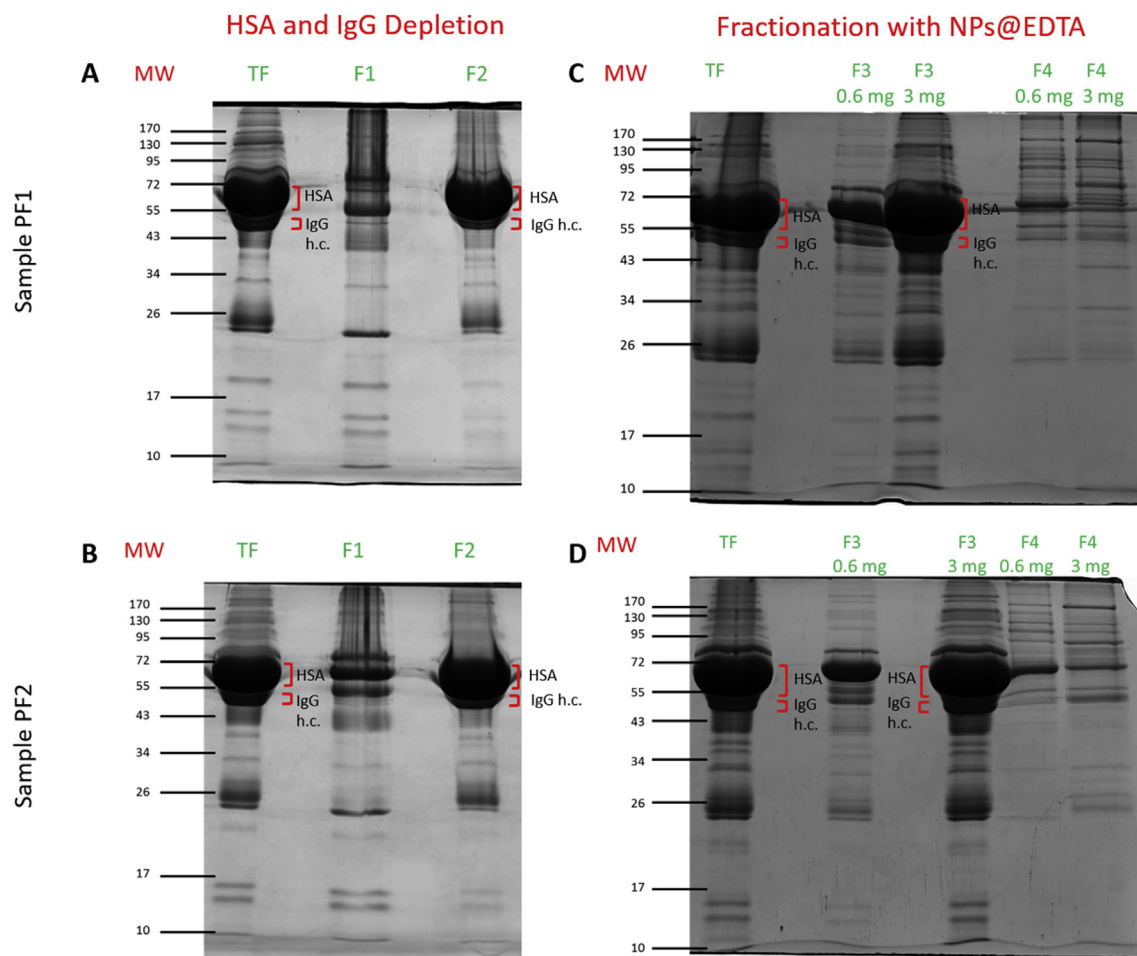


Fig. 2. SDS-PAGE profiles of the protein fractions collected with the commercial kit (A and B) and with the NPs@EDTA (C and D), from two individuals (top: PF1, bottom: PF2). The first lane in each gel (TF) corresponds to the total/unprocessed sample. F1: albumin (HSA)/IgG-poor fraction; F2: HSA/IgG-rich fraction; F3: non-adsorbed fraction; F4: adsorbed fraction. Red brackets mark HSA and IgG heavy chain (h.c.) bands. (For interpretation of the references to colour in this figure legend, the reader is referred to the web version of this article.)

the adsorbed protein fraction (F4). These data suggest we are facing biological rather than technical proteome variations.

3.4. Saturation of NPs@EDTA with large volumes of PF increased proteome coverage

Aiming to find the saturation point of NPs@EDTA we repeated the experience, using the same amount of nanoparticles (1 mg), but with increasing amounts of PF protein: 0.3 mg, 1.5 mg, 3 mg and 4.5 mg. Fig. 4 depicts the SDS-PAGE profile of the adsorbed protein fractions collected in the saturation assay for sample PF2 (the same can be found in Figure S3 for PF1). As one can see, there is a gradual increase in nanoparticle saturation, as proven by similar intensities of gel bands across different samples with concomitant increase of starting protein mass. For instance, when one compares the assays with 3 mg and 4.5 mg, it is noticeable that bands B (~80 kDa), D (~40 kDa) and E (~35 kDa) display similar intensity across two lanes. Additionally, if one compares the assays with 1.5 mg and 3 mg, the same is true for bands A (~170 kDa) and C (~65–72 kDa). Thus, the main differences in bands' intensity are found when we compare the profiles respective to 0.3 mg and 1.5 mg. For instance, band D is nearly absent and bands A, B and E are fainter when processing only 0.3 mg of protein. Together, these data suggest that 1 mg NPs@EDTA can process up to 3 mg of PF proteins.

Despite the saturation of 1 mg of NPs@EDTA with 3 mg of protein, we sought to see if processing a large excess of PF (4.5 mg) would still increase PF proteome coverage and dynamic range. Thus, the proteins belonging to the adsorbed protein fraction were identified in the assay with 4.5 mg of initial protein. Curiously, we could identify again 185 proteins across the two individuals (Figure S4), with similar inter-individual variability – 66% versus 60% in the preliminary assay (Table 1). Although, we could explore a higher range of protein abundances (5.4 log units), outperforming the direct PF analysis, i.e. without fractionation/depletion steps. Furthermore, we could increase the total number of proteins identified to 247.

3.5. Reproducibility analysis of the NPs@EDTA-based fractionation method

Once the saturation point for the NPs@EDTA was calculated, we sought to see if the present method was reproducible. Thus, 3 mg of protein of the third PF sample (PF3) was fractionated with the NPs@EDTA in duplicate. The non-adsorbed fraction was then digested in solution and the peptides were analyzed by a more powerful MS instrument (LTQ-Orbitrap Velos Pro). Overall, 475 proteins could be identified (397 proteins in the first run and 399 proteins in the second run), with 68% of the proteins being

Table 1
Main indicators of proteome data, namely inter-individual variability, proteome coverage and increment of protein identification in comparison to total unprocessed samples.

General Statistics			
Total Number of Identified Proteins		185	
Total Number of Identified Proteins on Sample PF1		157	
Total Number of Identified Proteins on Sample PF2		150	
Number of Shared Proteins		122	Total Fraction (unprocessed samples)
Proteins shared between individuals		66%	Total Number of Proteins
			Proteins shared between individuals
			64%
Method 1: Depletion of HSA and IgG			
HSA- and IgG-rich fraction (F2)			HSA- and IgG-poor fraction (F1)
Total Number of Proteins		78	Total Number of Proteins
Proteins shared between individuals		41%	Proteins shared between individuals
Number of proteins identified exclusively by the method [in comparison to "Total Fraction"]			44
Increment of Protein Identification			29%
Method 2: Enrichment with NPs@EDTA			
Non-adsorbed protein fraction (F3)			Adsorbed protein fraction (F4)
Total Number of Proteins		86	Total Number of Proteins
Proteins shared between individuals		56%	Proteins shared between individuals
Number of proteins identified exclusively by the method [in comparison to "Total Fraction"]			46
Increment of Protein Identification			31%
Comparison between Methods			
Method 1: Depletion of HSA and IgG			Method 2: Enrichment with NPs@EDTA
Total Number of Proteins		140	Total Number of Proteins
Unique Number of Proteins		23	Unique Number of Proteins
Unique Coverage		12%	Unique Coverage
Increment of Protein Identification		38%	Increment of Protein Identification
Combined Coverage			37%
Combined Increment of Protein Identification			59%

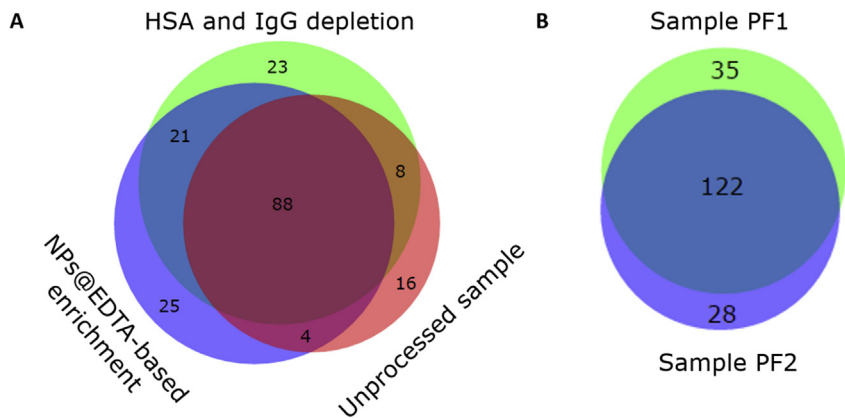


Fig. 3. Venn's graphical representation of the identified PF proteins (A) across the two approaches and unprocessed sample, and (B) across the two individuals.

Table 2
Dynamic range estimative (\log_{10} of the peptide intensity sum for each protein identified) for proteome data obtained from total unprocessed samples, fraction 1 (albumin/IgG-poor fraction) and 4 (NPs@EDTA-adsorbed protein fraction); this last in both the standard and in the saturation assays.

Fraction	\log_{10} Peptide Intensity Sum Range	$\Delta \log_{10}$
Total	1.5–6.3	4.8
F1	1.9–5.6	3.7
F4 (standard assay)	1.0–5.5	4.5
F4 (saturation assay)	1.2–6.6	5.4

identified in both MS/MS runs. Moreover, if one considers the proteins identified with higher confidence (i.e., with 2 or more peptides identified, as in the case of Xiang's work [5]), one can see that 82% of the proteome can be reproducibly identified (271 and 249 proteins identified in the first and second runs, respectively).

3.6. Gene ontology analysis

In order to compare protein localization as well as the biological processes between methods we performed a gene ontology (GO)-enrichment analysis. To predict protein localization, we used STRING webtool (Table S1). As expected, both methods allow to explore mainly secreted proteins, as exemplified by "extracellular space" and "extracellular exosome" GO terms. Besides, we used ClueGO, to get a glimpse over potentially trackable biological processes (network depicted in Fig. 5). In this analysis, we have compared all the proteins identified exclusively in the desired fraction of each method, namely, F1 (24 proteins) and F4 (99 proteins), to those identified by both methods (100 proteins). Interestingly, all processes could be either screened by both methods (Figures S5A and S5B) or by NPs@EDTA-based fractionation alone (Figure S6). Relevant biological phenomena that can be studied using NPs@EDTA alone are, for instance, defense response to

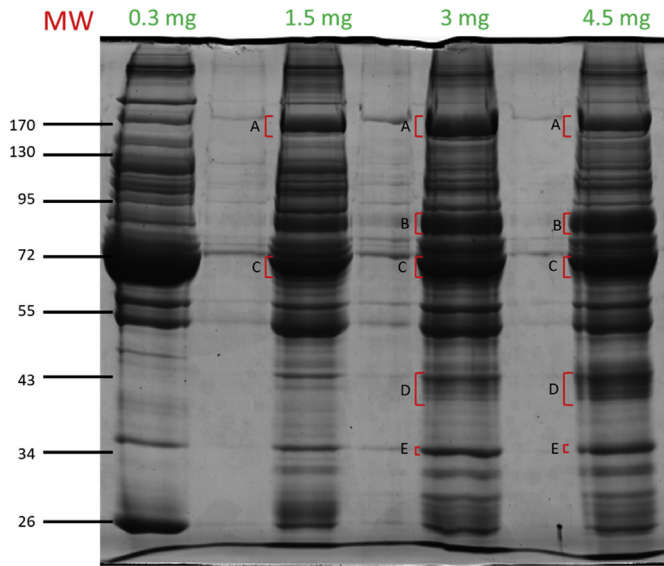


Fig. 4. SDS-PAGE profile of the adsorbed protein fractions retrieved after the processing of 0.3 mg, 1.5 mg, 3 mg and 4.5 mg of PF protein from sample PF2. Red brackets identify bands A to E, discussed in the text. (For interpretation of the references to colour in this figure legend, the reader is referred to the web version of this article.)

fungus, interleukin-8 production and low-density lipoprotein particle remodeling.

3.7. Comparison with known PF proteome

Overall 565 proteins were identified, representing 56% of those identified previously [5]. Still, more than half (297) of the identified proteins have not been previously assigned to PF. To analyze the proportion of plasma- and heart-derived proteins in PF's proteome, we have compared our dataset with that published by Farrah et al. [19] (cataloguing over 91 LC-MS/MS datasets) and by Aye et al. [20] (analyzing a healthy male's left ventricle tissue following several

fractionation, digestion and fragmentation strategies), respectively. When compared to the first PF's proteome reported, we found similar proportions of plasma proteins (62% versus 65%, $\Delta = 3\%$, n.s.) showing that NPs@EDTA platform does not induce a bias for the plasma subproteome. In turn, heart-derived proteins are slightly less represented (55% versus 62%, $\Delta = 7\%$, $p < 0.05$).

Aiming to retrieve the specific biological phenomena detectable with our dataset, we performed another GO analysis. For instance, we found that phenomena such as humoral immune response, regulation of plasma lipoproteins levels and response to wounding, among others, were more specifically associated to the proteins found in our dataset (Fig. 6 and Figure S7), showing that the molecular knowledge of this biofluid is far from being fully known.

4. Discussion

Owing to its anatomical distribution, the PF likely stores relevant molecular information reporting the pathophysiological status of the heart. However, the application of PF for diagnosis purposes is far from being a reality in everyday clinical routine. In fact, PF analysis is often limited to the determination of protein concentration, lactate dehydrogenase, adenosine deaminase (for the diagnosis of tuberculous pericarditis) and the search for malignant markers (such as carcinoembryonic antigen), when patients exhibit pericardial effusion [21]. Before the full exploitation of PF diagnostic properties, two major tasks superimpose, namely the complete characterization of PF's proteome and the development of suitable platforms for large-scale analysis. Xiang et al. [5] paved the way to fulfill the first, by performing the first in-depth PF proteomic characterization. In their work 1007 proteins were identified by pooling 10 PF samples from lung bullae patients and by performing two independent LC-MS/MS runs. Therefore, herein we describe a method to help complete the first task and to accomplish the second. We present an enrichment-based, instead of a depletion-based approach to characterize PF proteome, using affordable lab-made magnetic nanoparticles. Also, we have compared it to a commercially available method (albumin/IgG-depletion kit) in order to validate the use of NPs@EDTA for PF's proteome fractionation and characterization.

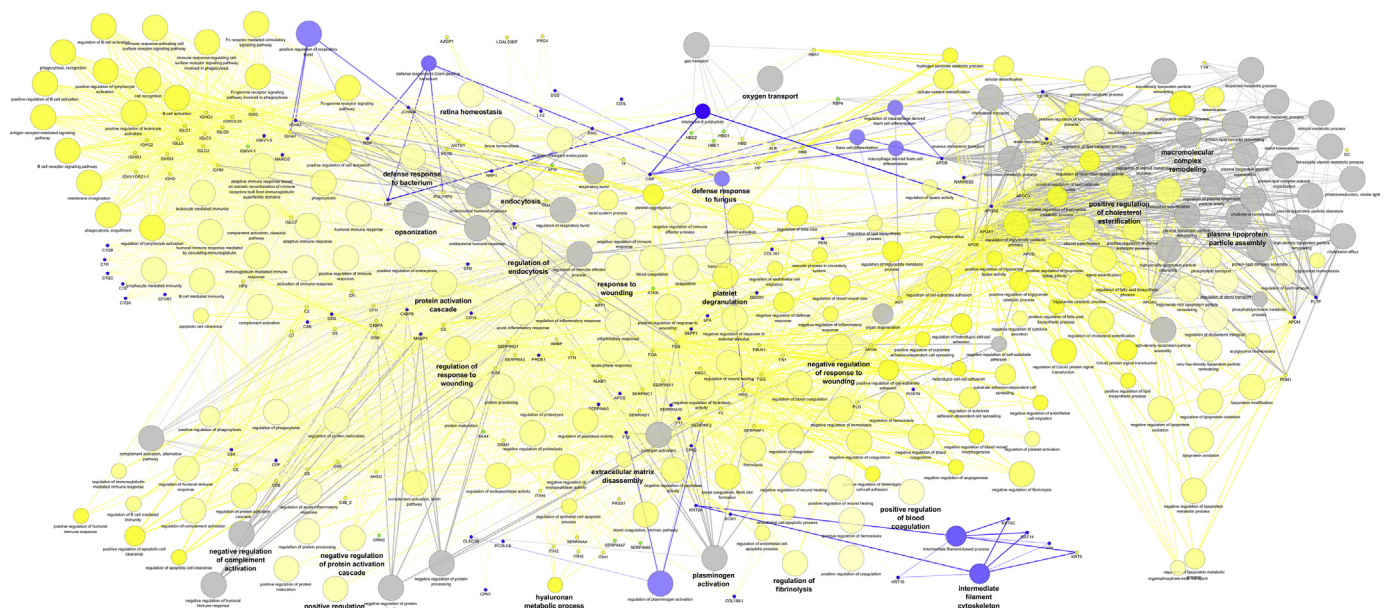


Fig. 5. ClueGO + CluePedia network depicting the main biological processes and related genes/proteins identified through the kit (green nodes), the NPs@EDTA (blue nodes) or both (yellow nodes). Gray nodes represent unspecific GO terms. Node size is proportional to each biological phenomenon's relevance. (For interpretation of the references to colour in this figure legend, the reader is referred to the web version of this article.)

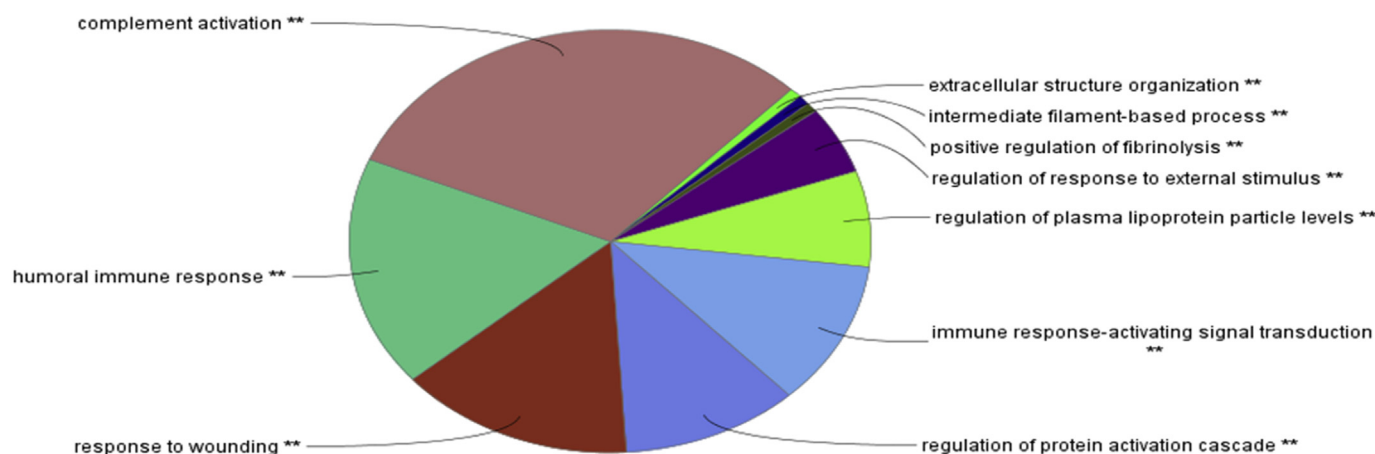


Fig. 6. Significant annotated biological processes associated to the experimental dataset as compared to Xiang's et al. [5].

The first challenge in the characterization of PF is, similarly to plasma/serum, the high content in albumin [3]. Thus, proteome fractionation is imperative when one seeks to screen PF's proteome. In fact, by SDS-PAGE, we noticed that, similarly to the commercial kit, fractionating PF with NPs@EDTA decreased the amount of albumin and IgG. By doing so, the NPs@EDTA, like the antibody-based depletion method, increase the odds of identifying other less abundant proteins/peptides, usually uncovered. Moreover, NPs@EDTA-based fractionation exhibited reproducibility as corroborated by the presence of the same lane profiles while increasing the protein amount from 0.6 mg to 3 mg (Fig. 2C and D) as well as in the saturation assay (Fig. 4). Furthermore, NPs@EDTA-based method allowed the identification of a similar number of proteins (138 vs. 140), increased equally (40% vs. 38%) the number of identifications in comparison to the kit, allowed to monitor a higher range of proteins with different abundances (differing somewhere between 10^5 and 10^6 -fold) and displayed similar inter-individual variability (60% vs. 62%). For all these reasons, we validate the use of NPs@EDTA to fractionate and characterize PF's proteome.

In order to determine the suitable amount of magnetic beads to process PF, a saturation assay was performed with increasing amounts of protein to the same amount of NPs@EDTA. We found that 1 mg of NPs@EDTA can process up to 3 mg of protein. In a previous assay with urine, we found a 1:1 ratio to be the most appropriate to enrich the low abundant urinary proteins (unpublished data). Such difference can be explained mainly by the difference in albumin content between the biofluids. In fact, albumin may reach 70% of the total protein content in PF [3], while in urine it represents only 25% [22]. Thus, a lower proportion of NPs@EDTA in PF is needed to collect less abundant proteins. One advantage of using these nanoparticles to fractionate PF prior to proteomic analysis is the chance to adjust the amount of the beads to the protein amount. Contrarily, the commercial columns are limited to 600 μ g of protein (~ 10 μ L of serum/plasma). Thus, if one aims to process larger amounts of protein (especially important when the goal is to characterize subproteomes, such as the phosphoproteome) the sample needs to be separated in different columns, increasing sample manipulation as well as the processing time. Additionally, with magnetic nanoparticles, one can rapidly remove unbound proteins upon application of an external magnetic field.

Another important aspect to evaluate when designing new proteome fractionation strategies is the reproducibility of the protein identification. Therefore, we have repeated the protocol in duplicate for another sample, using 1 mg of NPs@EDTA to process

3 mg protein (as this was found to be the saturation point of the magnetic beads). However, in this assay we used a more powerful MS instrument (LTQ Orbitrap Velos), so that the number of proteins identified could be increased and, thus, the knowledge of the PF proteome. With this approach an inter-run proteome reproducibility of 68% was achieved for overall proteome and of 82% for proteins identified with 2 or more peptides. A study using similar MS instrumentation (LTQ Orbitrap Velos) achieved comparable inter-run reproducibility when processing sera samples with 2 immunodepletion methods. When using the MARS14 system, 79–85% of the proteins (≥ 2 peptides) were consistently identified. In turn, with the Prot20 system, 76–84% of the proteins (≥ 2 peptides) were always identified [23]. Using the same criteria for protein identification, Xiang et al. [5] could achieve a reproducibility of 80% for the proteins identified in the 2 separate MS/MS runs. Thus, we conclude our method to display a fairly good reproducibility, with the proteomes differences being intrinsically associated with the LC-MS/MS technology applied.

The use of NPs@EDTA is also made valid by GO analysis. First, no relevant changes in cell localization were found between the two methods. Second, even though some proteins could only be identified through the kit [e.g. attractin (ATRN), hemoglobin subunit gamma-1 (HBG1) and subunit epsilon (HBE1)], all biological processes were tracked by NPs@EDTA (blue nodes in Fig. 5) or by both methods (yellow or gray nodes in Fig. 5). Theoretically, these data show that using NPs@EDTA to fractionate PF one may screen relevant phenomena played by PF proteins exclusively identified through the depletion approach and prompts it to high throughput applications. Furthermore, some relevant biological processes were exclusively tracked with NPs@EDTA, e.g. IL-8 production and LDL particle remodeling. The monitoring of these processes in PF can be important to answer questions raised by the scientific community, with the additional advantage of PF being closer to the heart and more likely reflecting the onset of cardiovascular diseases. For instance, tracking of IL-8 production can be important to investigate why low pre-operative levels of IL-8 are associated to increase risk of developing postpericardiotomy syndrome [24] and, on the opposite, why high levels of this cytokine can predict mortality of acute coronary syndrome patients [25]. Moreover, we may validate the usefulness of LDL-cholesterol/apoB serum ratio as a coronary artery disease (CAD) risk predictor [26], by collecting PF and analyzing the same ratio in CAD patients undergoing surgical interventions (e.g. coronary artery bypass graft).

Notwithstanding the ability of NPs@EDTA to replace the traditional kit-based method, both helped expand the known PF

proteome. Collectively, we could identify 565 proteins across the two methods and sample fractions and 53% of those (297 proteins) have not been described before [5], to the best of our knowledge. Moreover, we could track specific biological phenomena with our dataset, less represented or without representation in the referential proteome (Fig. 6), namely regulation of response to external stimulus, humoral immune response, response to wounding, positive regulation of fibrinolysis, regulation of protein activation cascade and regulation of plasma lipoprotein particle levels. This can be explained, at least in part, by the main disadvantage of MARS, in which not only the targeted proteins but others are indirectly removed (depletome) due to unspecific binding [4]. Also, such phenomena can also be explained by a larger number of proteins identified through our approaches playing such roles. It is possible that other proteins involved in the same processes were already identified [5] but they are not as representative of those processes as the ones we found. Additionally, even though MARS targets the 14 most abundant proteins in plasma/PF, removing up to 94% of the total protein mass [4], the protein dynamic range is not as high, as one would envision. In fact, while in the first proteomic study performed with this system the protein abundance ranged in about 6.4 log units, we, with an affordable system, could explore a set of proteins whose abundance ranged 5.4 log units. Besides, even targeting the proteins of low abundance, a similar representation of heart- and plasma-derived PF's subproteomes was achieved. Together, these observations demonstrate the application potential of NPs@EDTA in the clinical investigation.

The present work enrolled 3 PF samples, with the first 2 being analyzed by a Triple TOF spectrometer and the latter by a LTQ Orbitrap spectrometer. At the end of the first experiment 247 proteins were identified. At a first glance, this can be considered a limitation, as this is a small number when compared to the 1007 proteins identified by others [5]. However, one should realize that such authors made use of a mass analyzer with higher resolving power (LTQ-Orbitrap with 100,000–240,000 versus Triple TOF with 40,000) [27], besides performing two MS/MS runs (873 and 937 proteins were identified in the first and second runs, respectively). Indeed, when we used a similar strategy we had increased the number of identified proteins to 565, at the end of the second experiment. The remaining difference can be explained by the depletion of the 14 most abundant proteins found in plasma (and probably in PF) and also by the pooling of 10 samples from different individuals [5]. Hence, increasing the number of enrolled subjects would likely increase these numbers. Also, the identification of a similar number of proteins (138) as compared to a depletion strategy (employing a HSA- and IgG-depletion kit) similar to that reported in [5], allowing the identification of 140 proteins using the same experimental and instrumentation conditions, corroborates such findings. Additionally, because the samples were not pooled prior to LC-MS/MS analysis we can evaluate inter-individual variability and set a reference to future studies (60–66% of the proteins were shared between individuals, when using NPs@EDTA), which was not possible in the former. Moreover, we used PF from three patients with the same clinical background (aortic stenosis). Thus, it is likely that enrolling patients with different conditions (e.g. CAD, congenital heart disease) will diversify PF's proteome and even point out potential markers for such pathologies.

5. Conclusions

Taken together, our work validates the use of NPs@EDTA to characterize PF's proteome. NPs@EDTA can be especially useful in large-scale applications such as in cohort studies due to their easy handling and affordability. Furthermore, together with the commercial kit, we could expand the PF proteome in 297 proteins,

showing how obscure it still is and warranting PF analysis from patients with different clinical backgrounds.

Conflict of interest

The authors declare no conflict of interest.

Acknowledgments

The authors thank Portuguese Foundation for Science and Technology (FCT), European Union, Quadro de Referência Estratégico Nacional (QREN), Fundo Europeu de Desenvolvimento Regional (FEDER) and Programa Operacional Factores de Competitividade (COMPETE) for funding iBiMED (UID/BIM/04501/2013), UnIC (UID/IC/00051/2013), CNC (PTDC/NEU-NMC/0205/2012, UID/NEU/04539/2013) and CICECO (POCI-01-0145-FEDER-007679 and UID/CTM/50011/2013) research units as well as Rui Vitorino's (IF/00286/2015), Ana Daniel-da-Silva's (IF/00405/2014) and Fabio's Fellowship Grant (SFRH/BD/111633/2015). The authors thank also the National Mass Spectrometry Network (RNEM, REDE/1506/REM/2005) and project DOCnet (NORTE-01-0145-FEDER-000003), supported by Norte Portugal Regional Operational Programme (NORTE 2020), under the PORTUGAL 2020 Partnership Agreement, for funding this work.

The authors would also like to thank "CRG/UPF Proteomics Unit, Centre de Regulació Genòmica (CRG), Universitat Pompeu Fabra (UPF), 08003 Barcelona" for the analysis of the third PF sample. The CRG/UPF Proteomics Unit is part of the Spanish Platform of Molecular and Bioinformatics Resources (ProteoRed), Instituto de Salud Carlos III (PT13/0001)."

Appendix A. Supplementary data

Supplementary data related to this article can be found at <https://doi.org/10.1016/j.abb.2017.09.016>.

References

- [1] K. Vogiatzidis, S.G. Zarogiannis, I. Aidonidis, E.I. Solenov, P.-A. Molyvdas, K.I. Gourgoulis, C. Hatzoglou, Physiology of pericardial fluid production and drainage, *Front. Physiol.* 6 (2015) 62, <https://doi.org/10.3389/fphys.2015.00062>.
- [2] M. Fujita, M. Komeda, K. Hasegawa, Y. Kihara, R. Nohara, S. Sasayama, Pericardial fluid as a new material for clinical heart research, *Int. J. Cardiol.* 77 (2016) 113–118, [https://doi.org/10.1016/S0167-5273\(00\)00462-9](https://doi.org/10.1016/S0167-5273(00)00462-9).
- [3] S. Ben-Horin, A. Shinfeld, E. Kachel, A. Chetrit, A. Livneh, The composition of normal pericardial fluid and its implications for diagnosing pericardial effusions, *Am. J. Med.* 118 (2016) 636–640, <https://doi.org/10.1016/j.amjmed.2005.01.066>.
- [4] E. Gianazza, I. Miller, L. Palazzolo, C. Parravicini, I. Eberini, With or without you — proteomics with or without major plasma/serum proteins, *J. Proteomics* 140 (2016) 62–80, <https://doi.org/10.1016/j.jprot.2016.04.002>.
- [5] F. Xiang, X. Guo, W. Chen, J. Wang, T. Zhou, F. Huang, C. Cao, X. Chen, Proteomics analysis of human pericardial fluid, *Proteomics* 13 (2013) 2692–2695, <https://doi.org/10.1002/pmic.201200317>.
- [6] F. Trindade, F. Amado, R.P. Oliveira-Silva, A.L. Daniel-da-Silva, R. Ferreira, J. Klein, R. Faria-Almeida, P.S. Gomes, R. Vitorino, Toward the definition of a peptidome signature and protease profile in chronic periodontitis, *PROTEOMICS — Clin. Appl.* 9 (2015) 917–927, <https://doi.org/10.1002/prca.201400191>.
- [7] R. Oliveira-Silva, J. Pinto da Costa, R. Vitorino, A.L. Daniel-da-Silva, Magnetic chelating nanoprobe for enrichment and selective recovery of metalloproteases from human saliva, *J. Mat. Chem. B* 3 (2015) 238–249, <https://doi.org/10.1039/C4TB01189A>.
- [8] U.K. Laemmli, Cleavage of structural proteins during the assembly of the head of bacteriophage T4, *Nature* 227 (1970) 680–685, <https://doi.org/10.1038/227680a0>.
- [9] J.R. Wiśniewski, A. Zougman, N. Nagaraj, M. Mann, Universal sample preparation method for proteome analysis, *Nat. Methods* 6 (2009) 359–362, <https://doi.org/10.1038/nmeth.1322>.
- [10] S.I. Anjo, C. Santa, B. Manadas, Short GeLC-SWATH: a fast and reliable quantitative approach for proteomic screenings, *Proteomics* 15 (2015) 757–762, <https://doi.org/10.1002/pmic.201400221>.

- [11] C. Silva, C. Santa, S.I. Anjo, B. Manadas, A reference library of peripheral blood mononuclear cells for SWATH-MS analysis, *PROTEOMICS – Clin. Appl.* 10 (2016) 760–764, <https://doi.org/10.1002/prca.201600070>.
- [12] L. Sennels, J.-C. Bukowski-Wills, J. Rappsilber, Improved results in proteomics by use of local and peptide-class specific false discovery rates, *BMC Bioinforma.* 10 (2009) 1–11, <https://doi.org/10.1186/1471-2105-10-179>.
- [13] W.H. Tang, I.V. Shilov, S.L. Seymour, Nonlinear fitting method for determining local false discovery rates from decoy database searches, *J. Proteome Res.* 7 (2008) 3661–3667, <https://doi.org/10.1021/pr070492f>.
- [14] J.S. Cottrell, U. London, Probability-based protein identification by searching sequence databases using mass spectrometry data, *Electrophoresis* 20 (1999) 3551–3567, [https://doi.org/10.1002/\(SICI\)1522-2683\(19991201\)20:18<3551::AID-ELPS3551>3.0.CO;2-2](https://doi.org/10.1002/(SICI)1522-2683(19991201)20:18<3551::AID-ELPS3551>3.0.CO;2-2).
- [15] T. Hulsen, J. de Vlieg, W. Alkema, BioVenn – a web application for the comparison and visualization of biological lists using area-proportional Venn diagrams, *BMC Genomics* 9 (2008) 488, <https://doi.org/10.1186/1471-2164-9-488>.
- [16] D. Szklarczyk, A. Franceschini, S. Wyder, K. Forslund, D. Heller, J. Huerta-Cepas, M. Simonovic, A. Roth, A. Santos, K.P. Tsafou, M. Kuhn, P. Bork, L.J. Jensen, C. von Mering, STRING v10: protein-protein interaction networks, integrated over the tree of life, *Nucleic Acids Res.* 43 (2015) D447–D452, <https://doi.org/10.1093/nar/gku1003>.
- [17] G. Bindea, B. Mlecnik, H. Hackl, P. Charoentong, M. Tosolini, A. Kirilovsky, W.-H. Fridman, F. Pagès, Z. Trajanoski, J. Galon, ClueGO: a Cytoscape plug-in to decipher functionally grouped gene ontology and pathway annotation networks, *Bioinformatics* 25 (2009) 1091–1093, <https://doi.org/10.1093/bioinformatics/btp101>.
- [18] M. Page, R. Thorpe, Analysis of IgG fractions by electrophoresis, in: J.M. Walker (Ed.), *Protein Protoc. Handb.*, Humana Press, Totowa, NJ, 2002, pp. 1005–1007, <https://doi.org/10.1385/1-59259-169-8>, 1005.
- [19] T. Farrah, E.W. Deutsch, G.S. Omenn, D.S. Campbell, Z. Sun, J.A. Bletz, P. Mallick, J.E. Katz, J. Malmström, R. Ossola, J.D. Watts, B. Lin, H. Zhang, R.L. Moritz, R. Aebersold, A high-confidence human plasma proteome reference set with estimated concentrations in PeptideAtlas, *Mol. Cell. Proteomics* 10 (2011) 1–14, <https://doi.org/10.1074/mcp.M110.006353>.
- [20] T.T. Aye, A. Scholten, N. Taouatas, A. Varro, T.A.B. Van Veen, M.A. Vos, A.J.R. Heck, Proteome-wide protein concentrations in the human heart, *Mol. Biosyst.* 6 (2010) 1917–1927, <https://doi.org/10.1039/C004495D>.
- [21] L.J. Burgess, Biochemical analysis of pleural, peritoneal and pericardial effusions, *Clin. Chim. Acta* 343 (2004) 61–84, <https://doi.org/10.1016/j.cccn.2004.02.002>.
- [22] N. Nagaraj, M. Mann, Quantitative analysis of the intra- and inter-individual variability of the normal urinary proteome, *J. Proteome Res.* 10 (2011) 637–645, <https://doi.org/10.1021/pr100835s>.
- [23] M.P.W. Smith, S.L. Wood, A. Zougman, J.T.C. Ho, J. Peng, D. Jackson, D.A. Cairns, A.J.P. Lewington, P.J. Selby, R.E. Banks, A systematic analysis of the effects of increasing degrees of serum immunodepletion in terms of depth of coverage and other key aspects in top-down and bottom-up proteomic analyses, *Proteomics* 11 (2011) 2222–2235, <https://doi.org/10.1002/pmic.201100005>.
- [24] M. Jaworska-Wilczyńska, A. Magalska, K. Piwocka, P. Szymański, M. Kuśmierczyk, M. Wąsik, T. Hryniewiecki, Low interleukin - 8 level predicts the occurrence of the postpericardiotomy syndrome, *PLoS One* 9 (2014), <https://doi.org/10.1371/journal.pone.0108822> e108822.
- [25] E. Cavusoglu, J.D. Marmur, S. Yanamadala, V. Chopra, S. Hegde, A. Nazli, K.P. Singh, M. Zhang, C. Eng, Elevated baseline plasma IL-8 levels are an independent predictor of long-term all-cause mortality in patients with acute coronary syndrome, *Atherosclerosis* 242 (2015) 589–594, <https://doi.org/10.1016/j.atherosclerosis.2015.08.022>.
- [26] S. Tani, Y. Saito, T. Anazawa, H. Kawamata, S. Furuya, H. Takahashi, K. Iida, M. Matsumoto, T. Washio, N. Kumabe, K. Nagao, A. Hirayama, Low-density lipoprotein cholesterol/apolipoprotein B ratio may be a useful index that differs in statin-treated patients with and without coronary artery disease, *Int. Heart J.* 52 (2011) 343–347, <https://doi.org/10.1536/ihj.52.343>.
- [27] Z. Zhang, S. Wu, D.L. Stenoien, L. Paša-Tolić, High-throughput proteomics, *Annu. Rev. Anal. Chem.* 7 (2014) 427–454, <https://doi.org/10.1146/annurev-anchem-071213-020216>.